Electronic Supplementary Information

Degradable Polymer Prodrugs with Adjustable Activity from Drug-Initiated Radical Ring-Opening Copolymerization

Elise Guégain,[1] Johanna Tran,[1] Quentin Deguettes,[1] Julien Nicolas[1,]*

[1]Institut Galien Paris-Sud, UMR CNRS 8612, Univ Paris-Sud, Faculté de Pharmacie, 5 rue Jean-Baptiste Clément, F-92296 Châtenay-Malabry cedex, France.

*To whom correspondence should be addressed.

Email: julien.nicolas@u-psud.fr

Tel.: +33 1 46 83 58 53

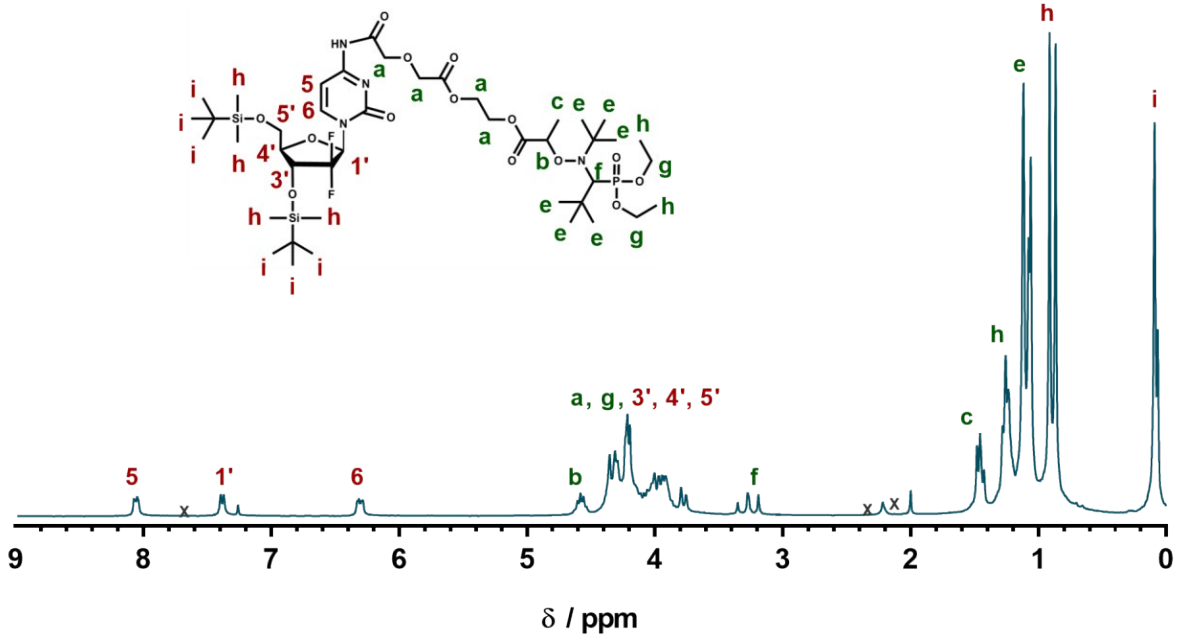

Figure S1. ^{1}H NMR spectrum in $CDCl_3$ in the 0–9 ppm region of Gem-digly-AMA-SG1.

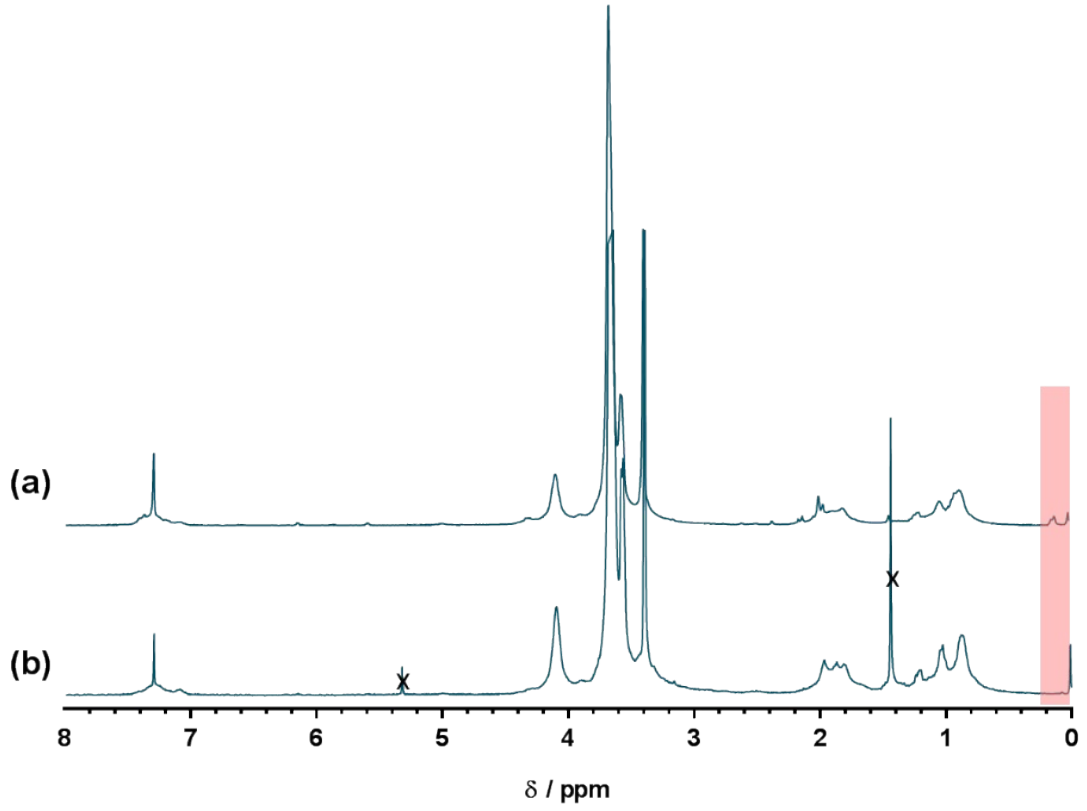

Figure S2. ^{1}H NMR spectrum in $CDCl_3$ in the 0–8 ppm region of Gem-digly-P(OEGMA-*co*-MPDL) **P2d** ($f_{MPDL,0}$ = 0.4), (a) after one precipitation and before deprotection and (b) after deprotection. The colored area shows the TBDMS group and its removal after deprotection.

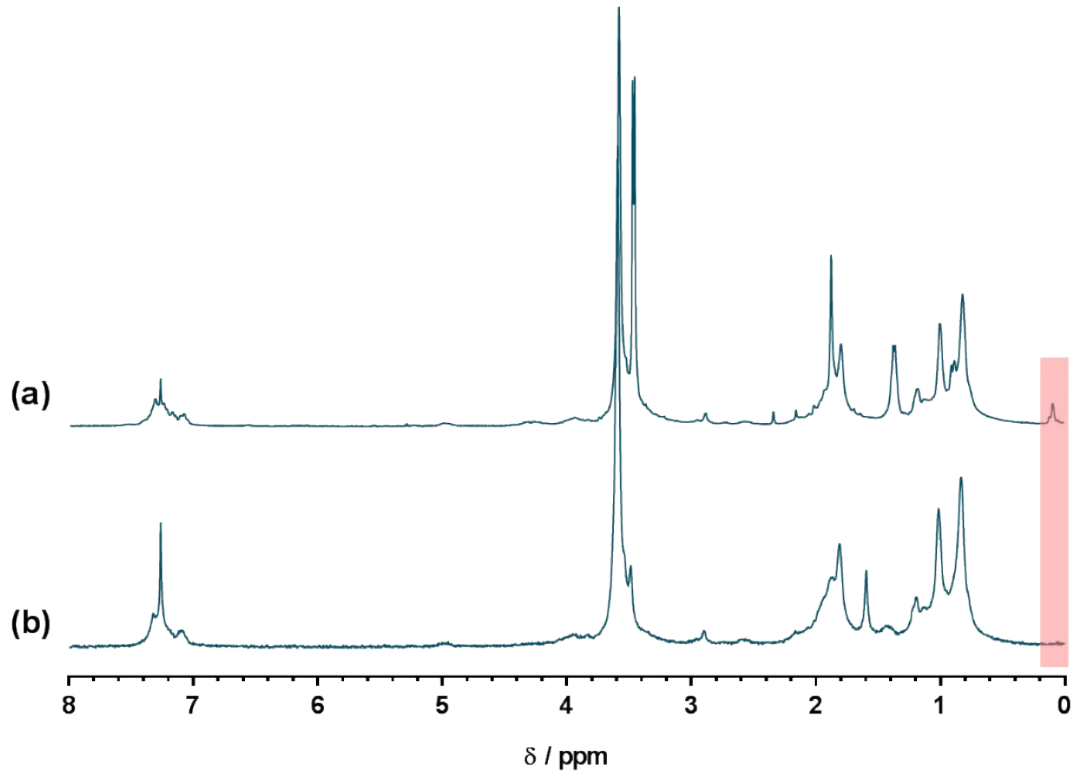

Figure S3. ^{1}H NMR spectrum in $CDCl_3$ in the 0–8 ppm region of Gem-digly-P(MMA-*co*-MPDL) **P5d** ($f_{MPDL,0}$ = 0.4), (a) after one precipitation and before deprotection and (b) after deprotection. The colored area shows the TBDMS group and its removal after deprotection.

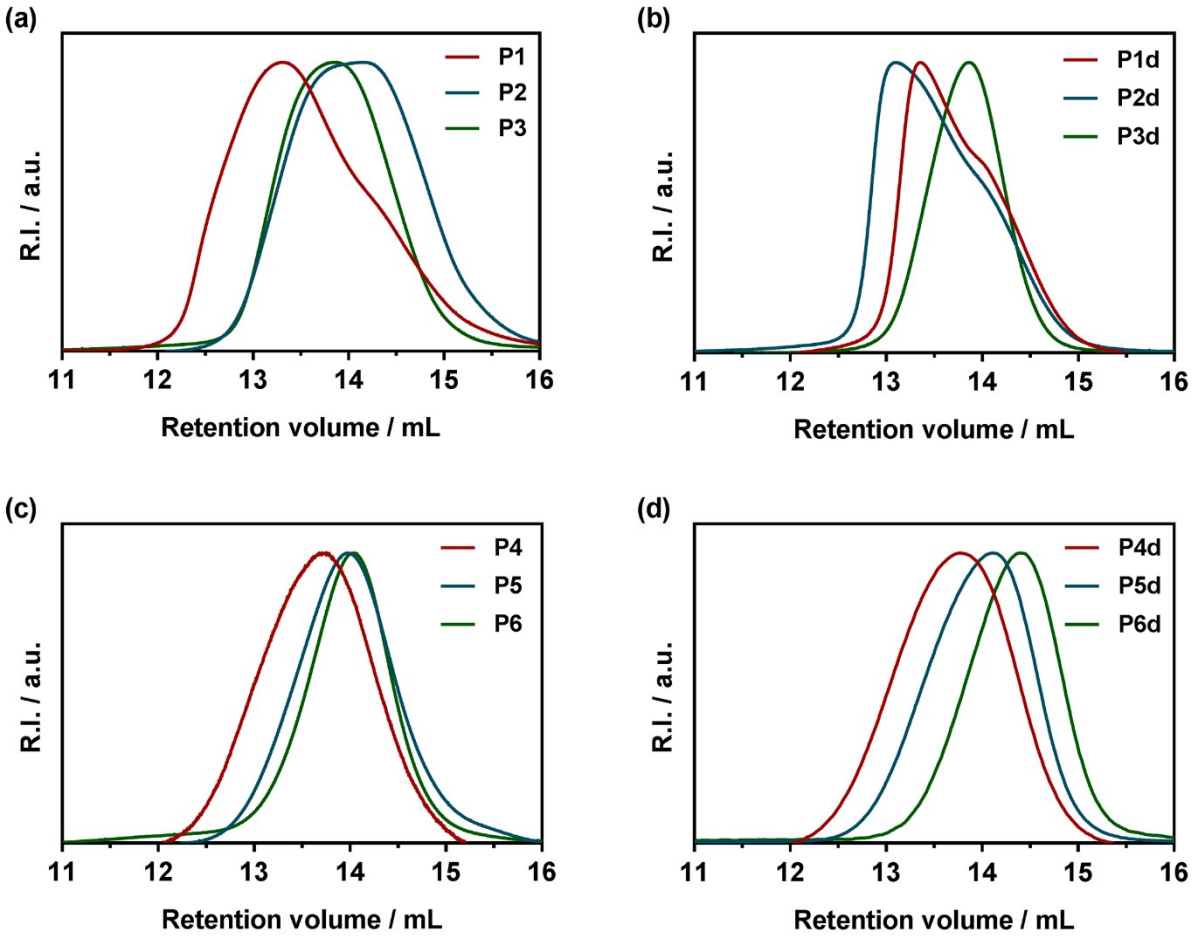

Figure S4. Size exclusion chromatograms ($CHCl_3$ eluent, 1 $mL.min^{-1}$) of (a) Gem-P(OEGMA-*co*-MPDL), **P1–P3**, (b) Gem-digly-P(OEGMA-*co*-MPDL), **P1d–P3d**, (c) Gem-P(MMA-*co*-MPDL), **P4–P6** and (d) Gem-digly-P(MMA-*co*-MPDL), **P4d–P6d**.

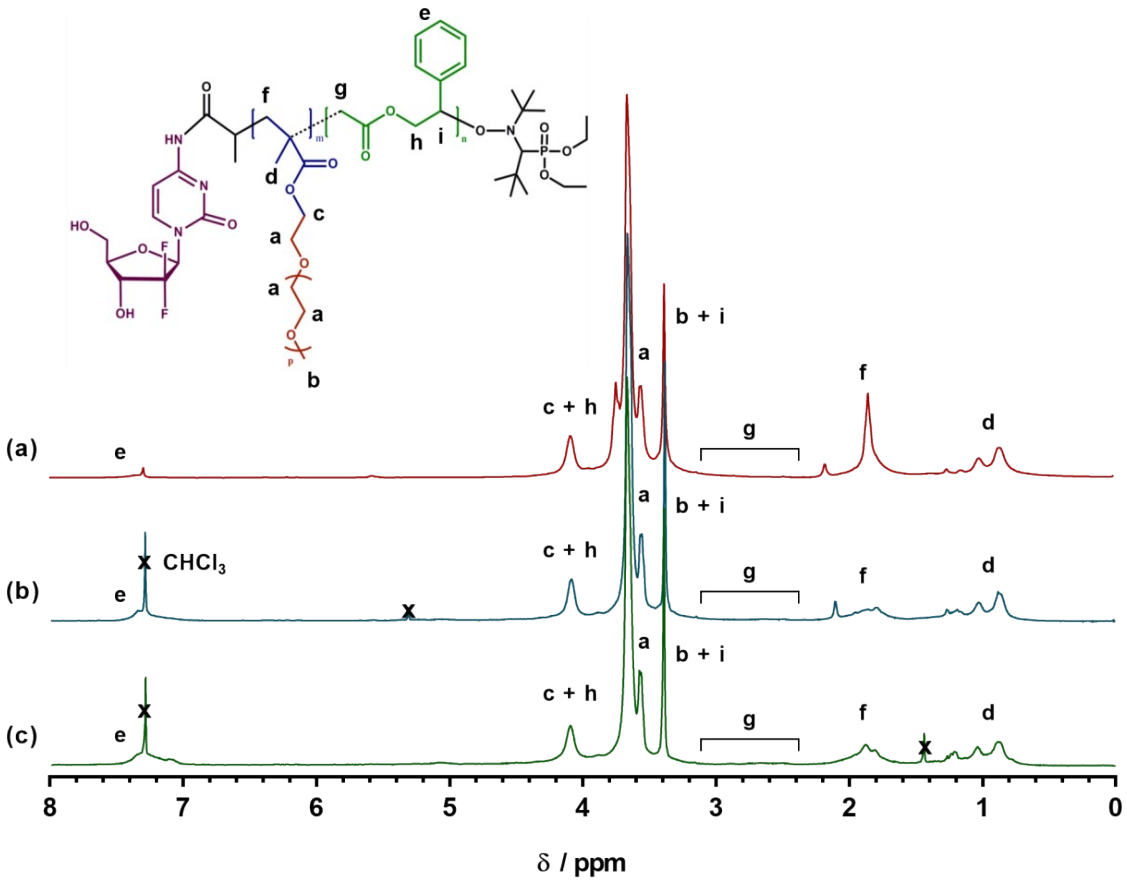

Figure S5. ^{1}H NMR spectra in $CDCl_3$ in the 0–8 ppm region of Gem-P(OEGMA-*co*-MPDL) with (a) **P1** ($f_{MPDL,0} = 0.2$); (b) **P2** ($f_{MPDL,0} = 0.4$); (c) **P3** ($f_{MPDL,0} = 0.7$).

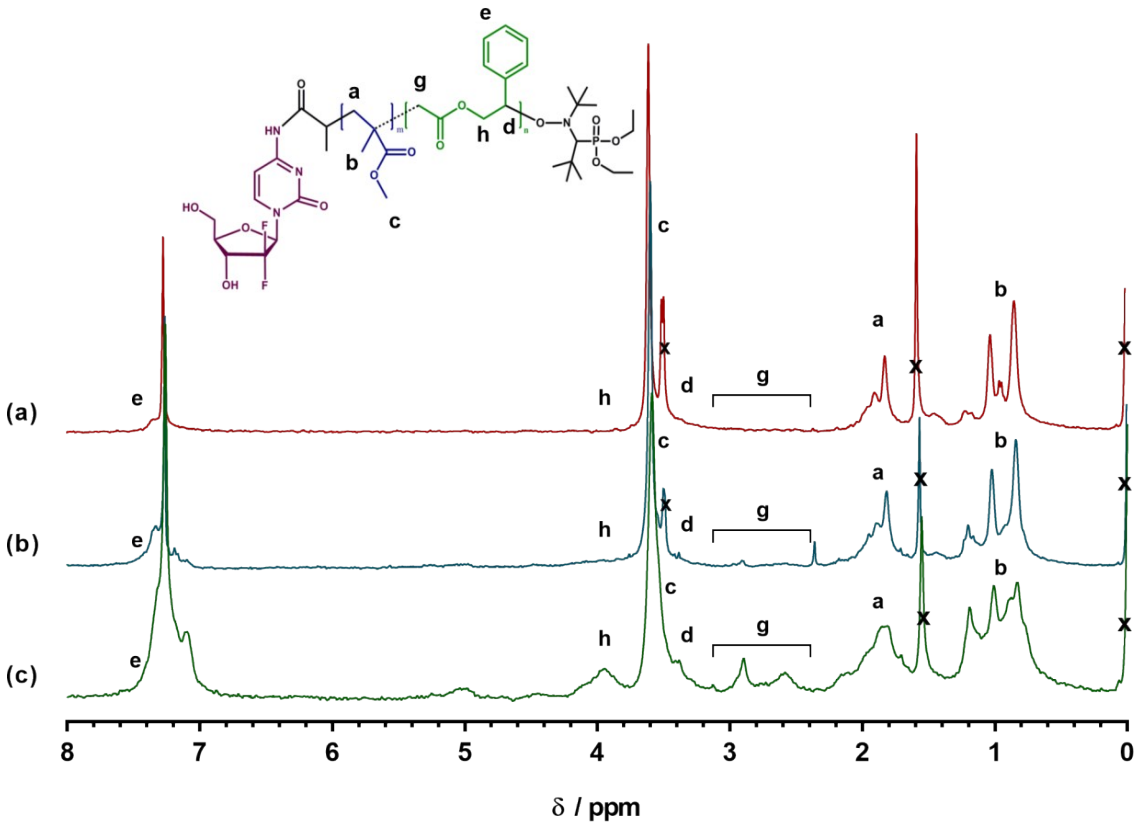

Figure S6. ^{1}H NMR spectra in $CDCl_3$ in the 0-8 ppm region of Gem-P(MMA-*co*-MPDL) with (a) **P4** ($f_{MPDL,0}$ = 0.2); (b) **P5** ($f_{MPDL,0}$ = 0.4); (c) **P6** ($f_{MPDL,0}$ = 0.7).

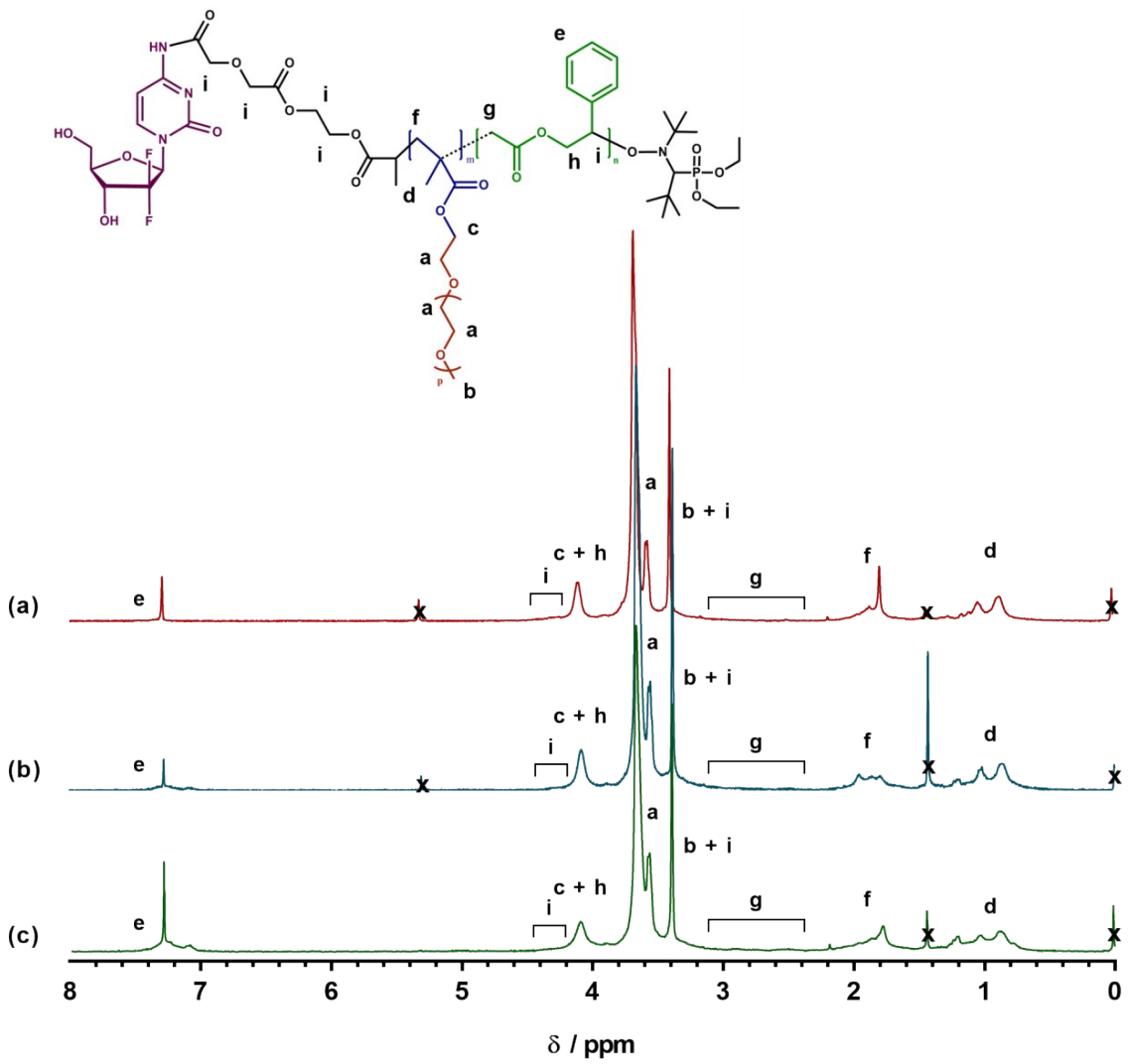

Figure S7. ^{1}H NMR spectra in $CDCl_3$ in the 0–8 ppm region of Gem-digly-P(OEGMA-*co*-MPDL) with (a) **P1d** ($f_{MPDL,0}$ = 0.2); (b) **P2d** ($f_{MPDL,0}$ = 0.4); (c) **P3d** ($f_{MPDL,0}$ = 0.7).

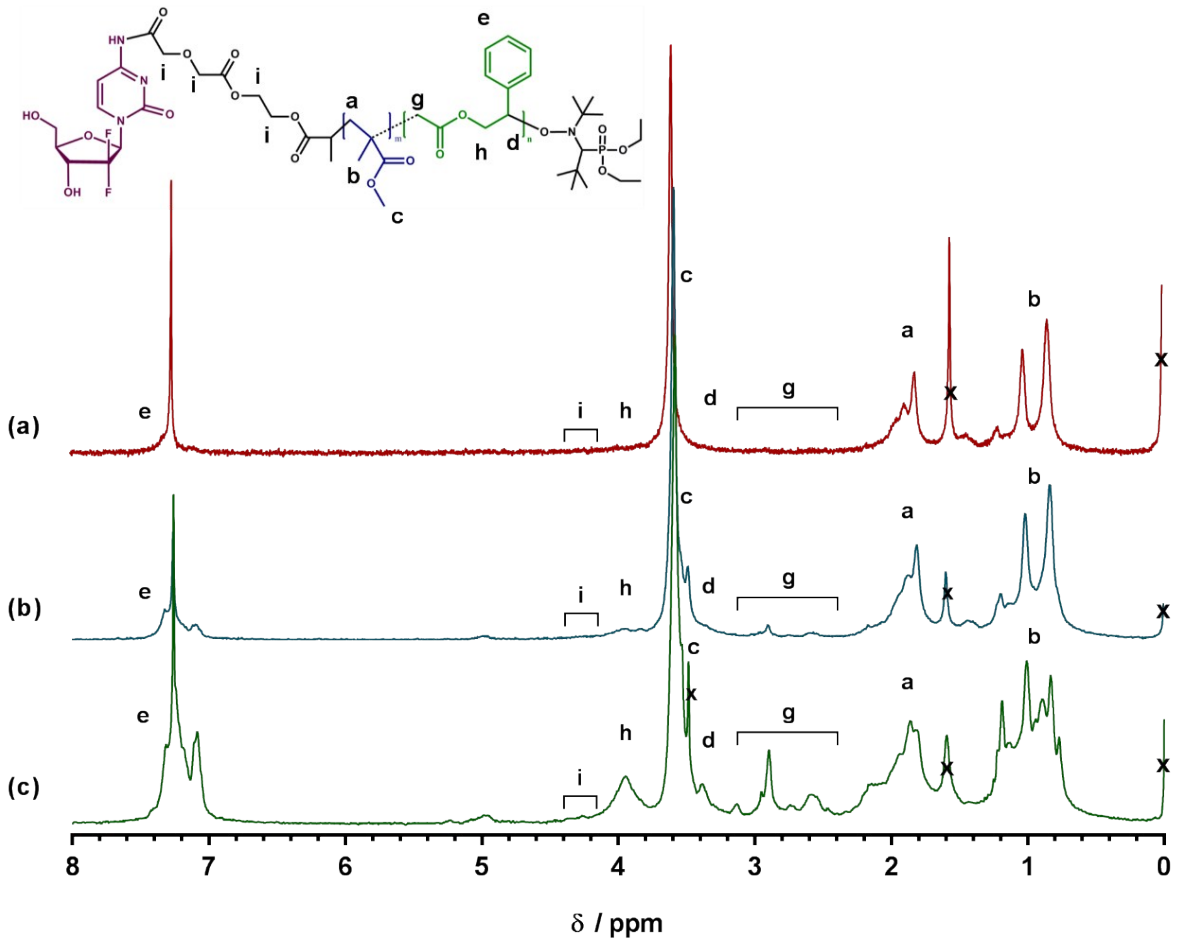

Figure S8. ^{1}H NMR spectra in $CDCl_3$ in the 0–8 ppm region of Gem-digly-P(MMA-*co*-MPDL) with (a) **P4d** ($f_{MPDL,0}$ = 0.2); (b) **P5d** ($f_{MPDL,0}$ = 0.4); (c) **P6d** ($f_{MPDL,0}$ = 0.7).

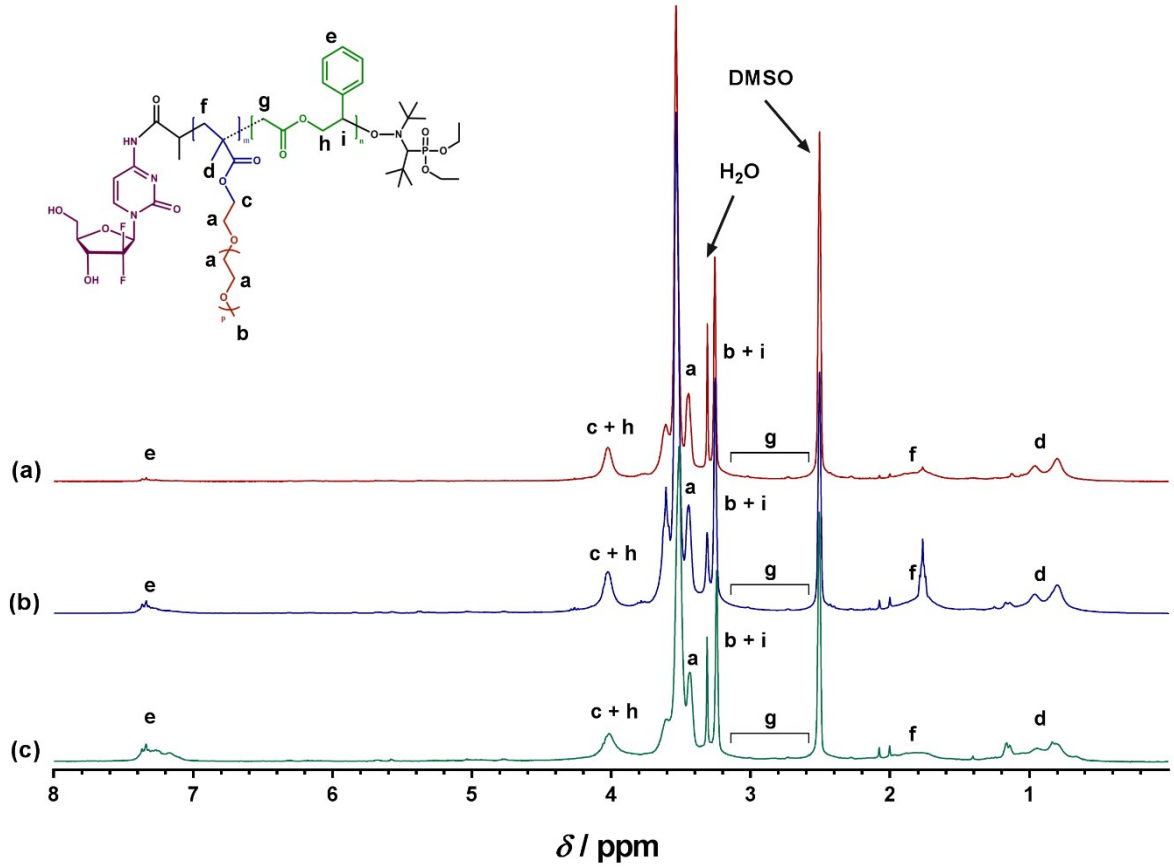

Figure S9. ^{1}H NMR spectra in DMSO-d_6 in the 0–8 ppm region of Gem-P(OEGMA-*co*-MPDL) with (a) **P1** ($f_{MPDL,0}$ = 0.2); (b) **P2** ($f_{MPDL,0}$ = 0.4); (c) **P3** ($f_{MPDL,0}$ = 0.7).

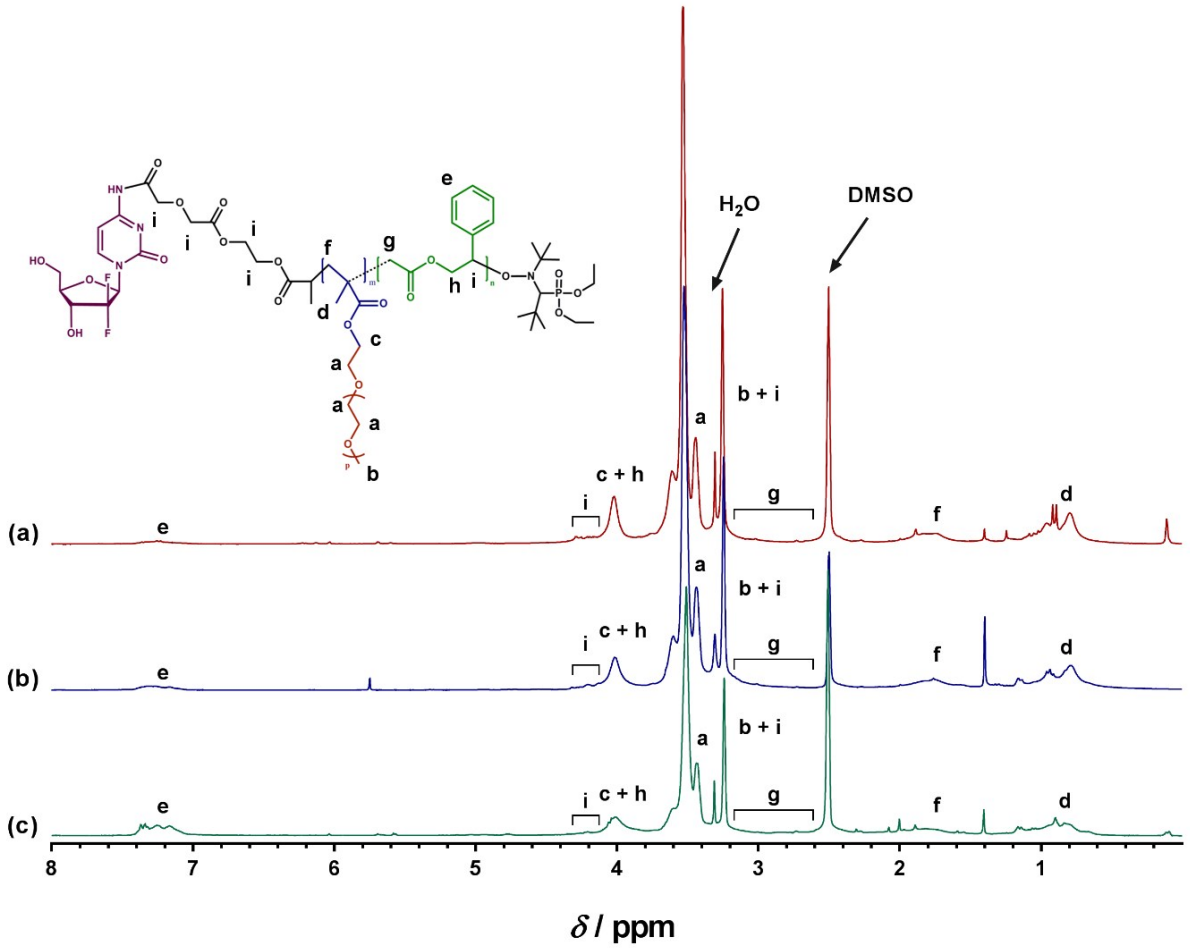

Figure S10. ^{1}H NMR spectra in DMSO-d_6 in the 0-8 ppm region of Gem-P(MMA-*co*-MPDL) with (a) **P4** ($f_{MPDL,0}$ = 0.2); (b) **P5** ($f_{MPDL,0}$ = 0.4); (c) **P6** ($f_{MPDL,0}$ = 0.7).

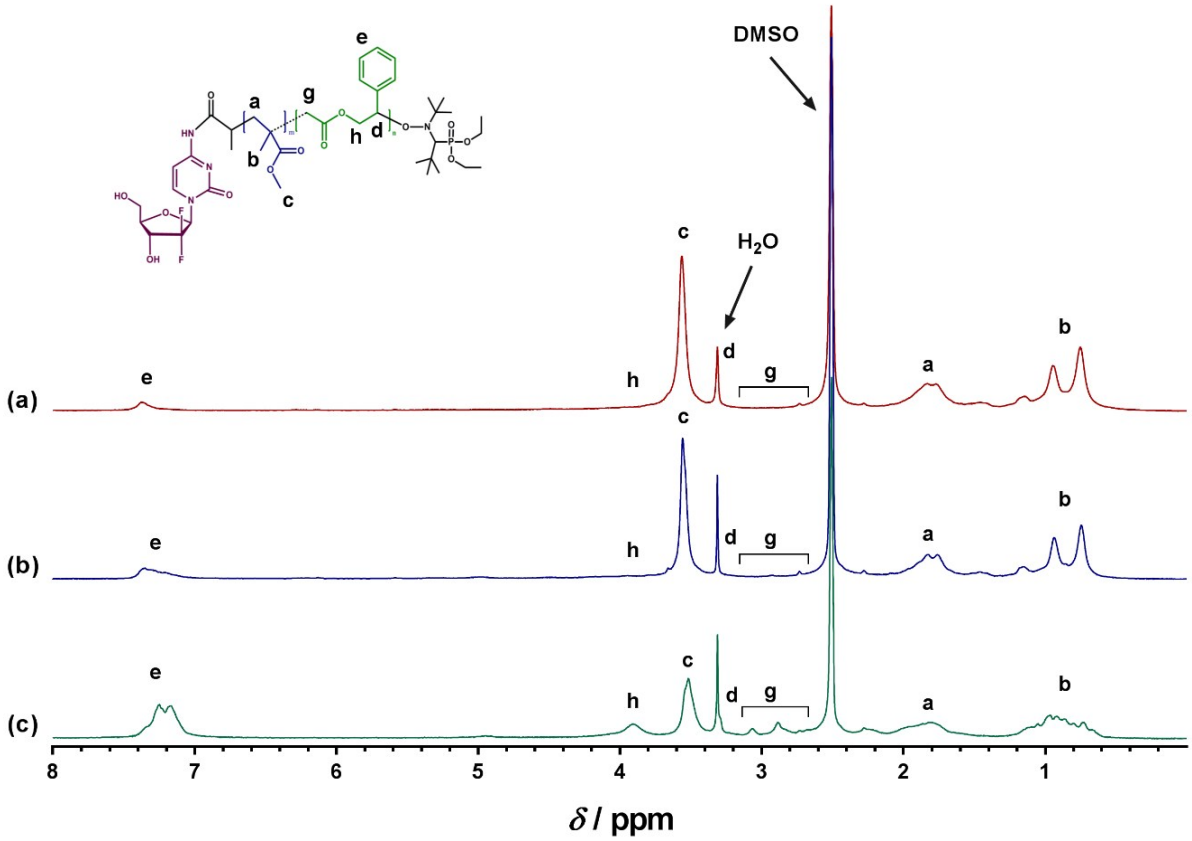

Figure S11. ^{1}H NMR spectra in DMSO-d_6 in the 0–8 ppm region of Gem-digly-P(OEGMA-*co*-MPDL) with (a) **P1d** ($f_{MPDL,0}$ = 0.2); (b) **P2d** ($f_{MPDL,0}$ = 0.4); (c) **P3d** ($f_{MPDL,0}$ = 0.7).

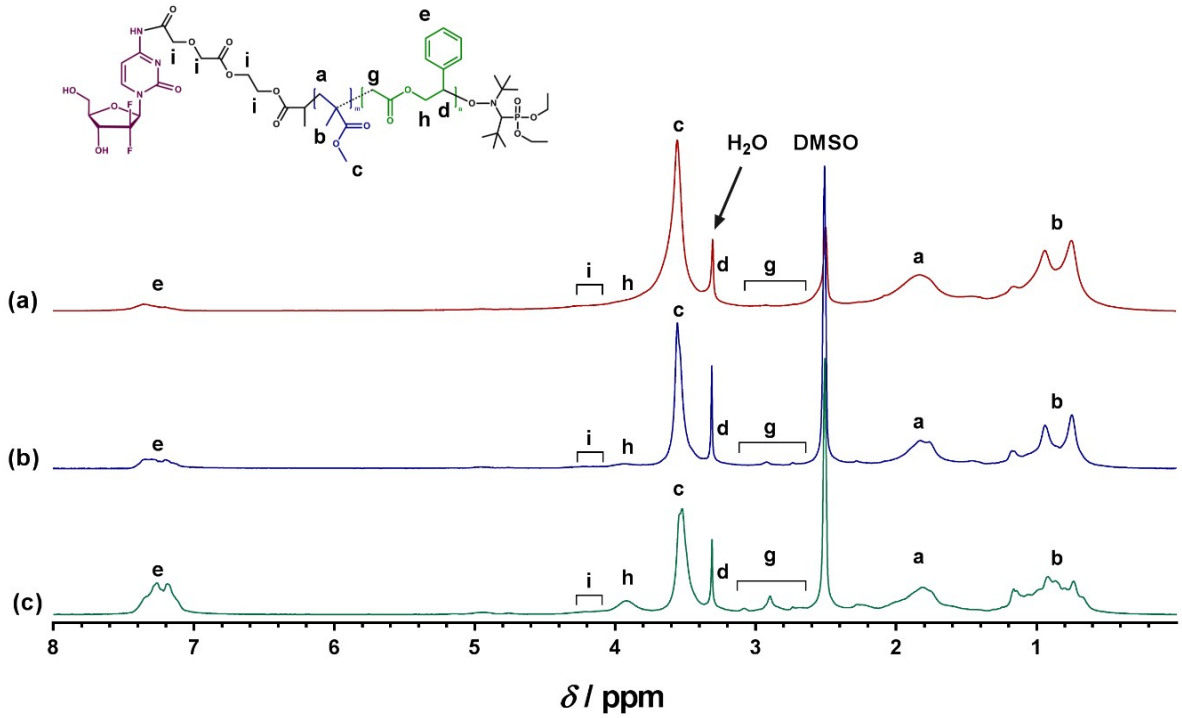

Figure S12. ^{1}H NMR spectra in DMSO-d_6 in the 0–8 ppm region of Gem-digly-P(MMA-*co*-MPDL) with (a) **P4d** ($f_{MPDL,0}$ = 0.2); (b) **P5d** ($f_{MPDL,0}$ = 0.4); (c) **P6d** ($f_{MPDL,0}$ = 0.7).

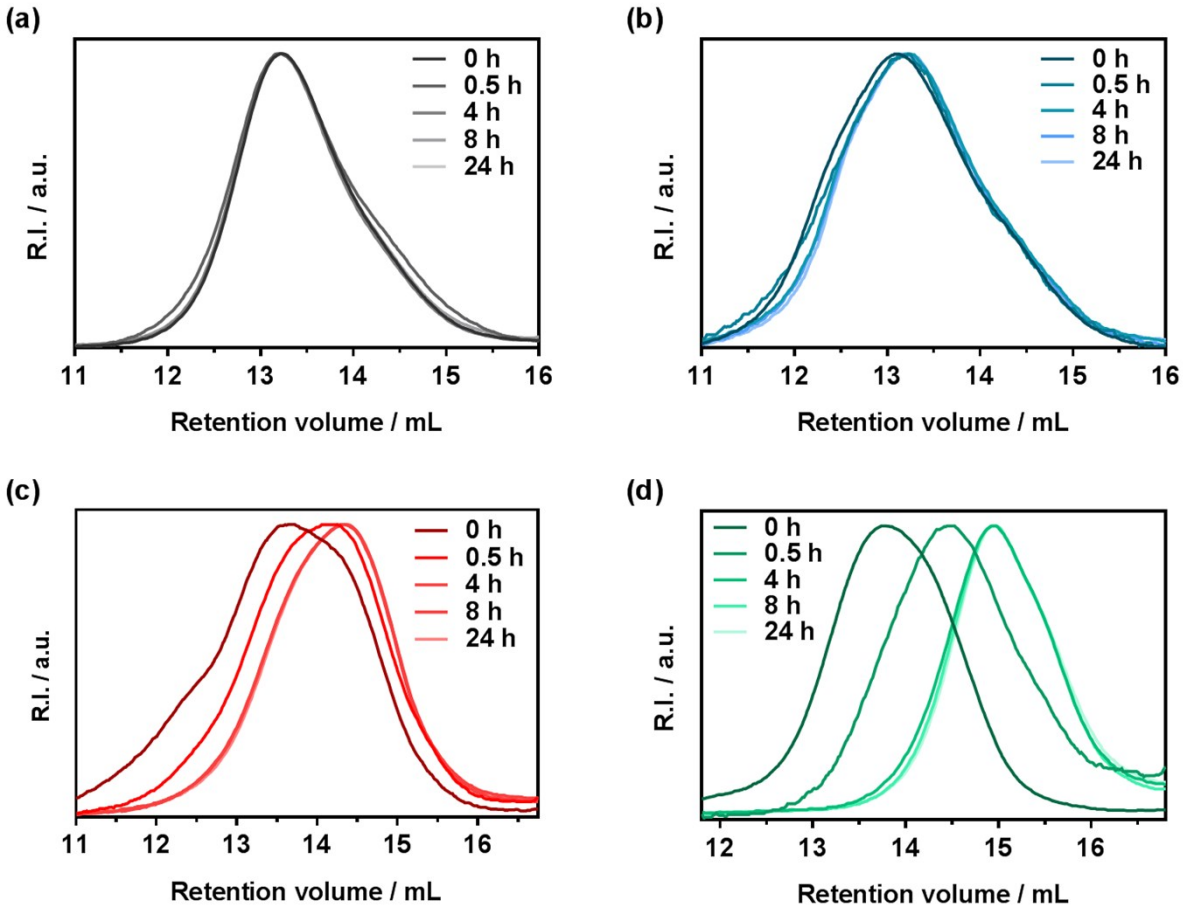

Figure S13. Evolution of the SEC chromatograms at different time during the hydrolytic degradation under accelerated conditions (KOH 5%) of Gem-P(OEGMA-*co*-MPDL) as function of the MPDL content: (a) ●, control (F_{MPDL} = 0); (b) ▲, **P1** (F_{MPDL} = 0.06); (c) ■, **P2** (F_{MPDL} = 0.12); (d) ▼, **P3** (F_{MPDL} = 0.25).

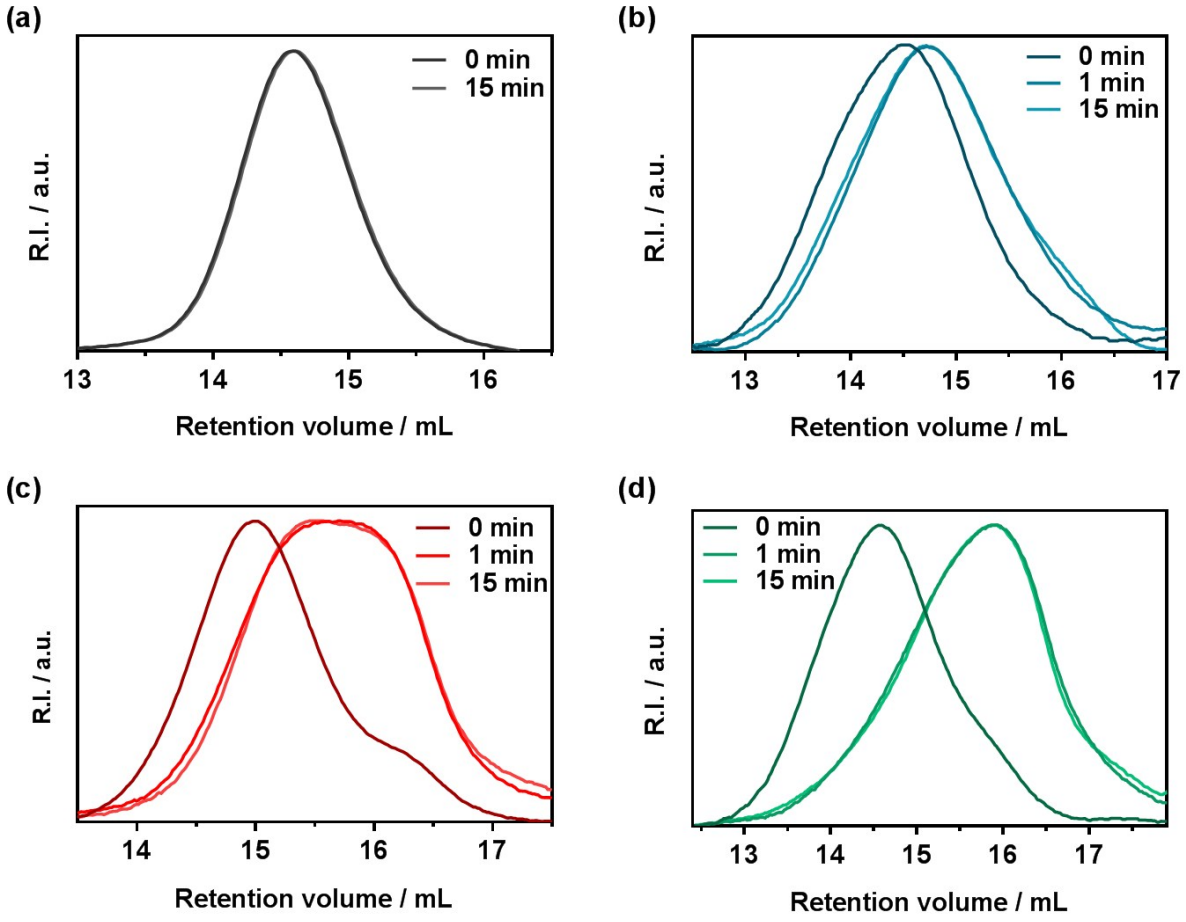

Figure S14. Evolution of the SEC chromatograms at different time during the hydrolytic degradation under accelerated conditions (KOH 5%) of Gem-P(MMA-*co*-MPDL) as function of the MPDL content: (a) ●, control (F_{MPDL} = 0); (b) ▲, **P4** (F_{MPDL} = 0.06); (c) ■, **P5** (F_{MPDL} = 0.12); (d) ▼, **P6** (F_{MPDL} = 0.25).

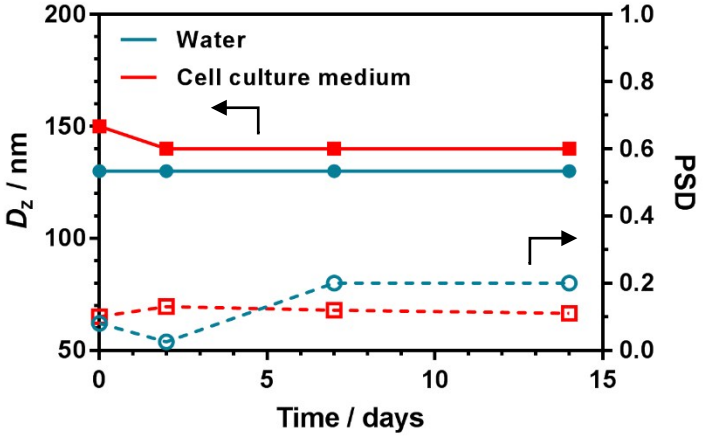

Figure S15. Evolution with time of the average diameter and the particle size distribution (PSD) of Gem-P(MMA-*co*-MPDL) (**P6**) nanoparticles in water and in cell culture medium determined by DLS.

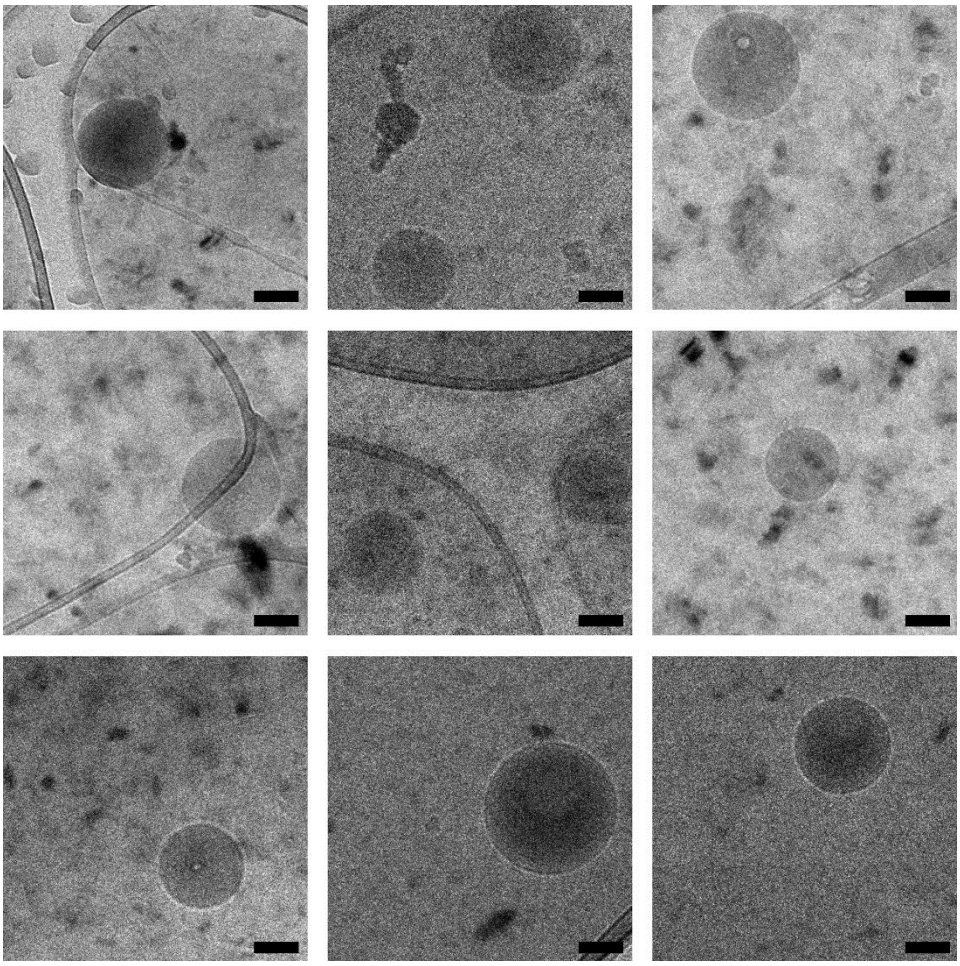

Figure S16. Representative Cryo-TEM images of Gem-P(MMA-*co*-MPDL) **P6** nanoparticles. Scale bar = 100 nm.

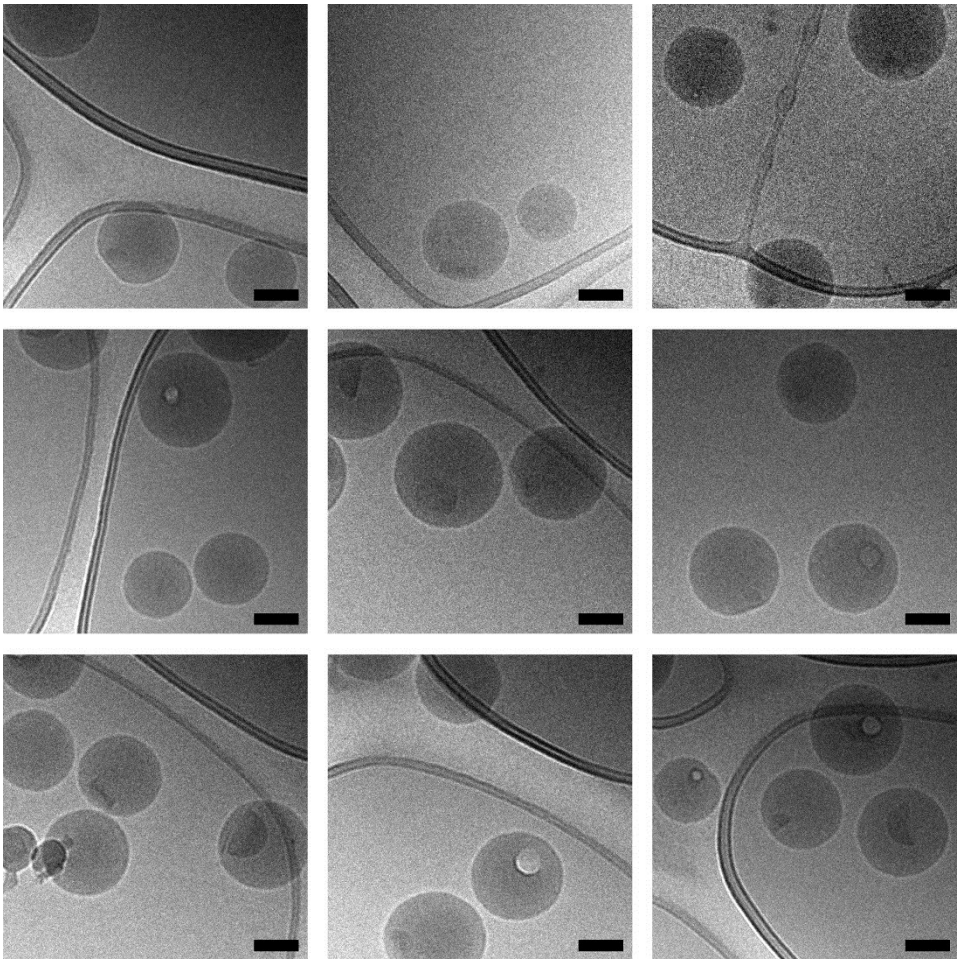

Figure S17. Representative Cryo-TEM images of Gem-digly-P(MMA-*co*-MPDL) **P6d** nanoparticles. Scale bar = 100 nm.

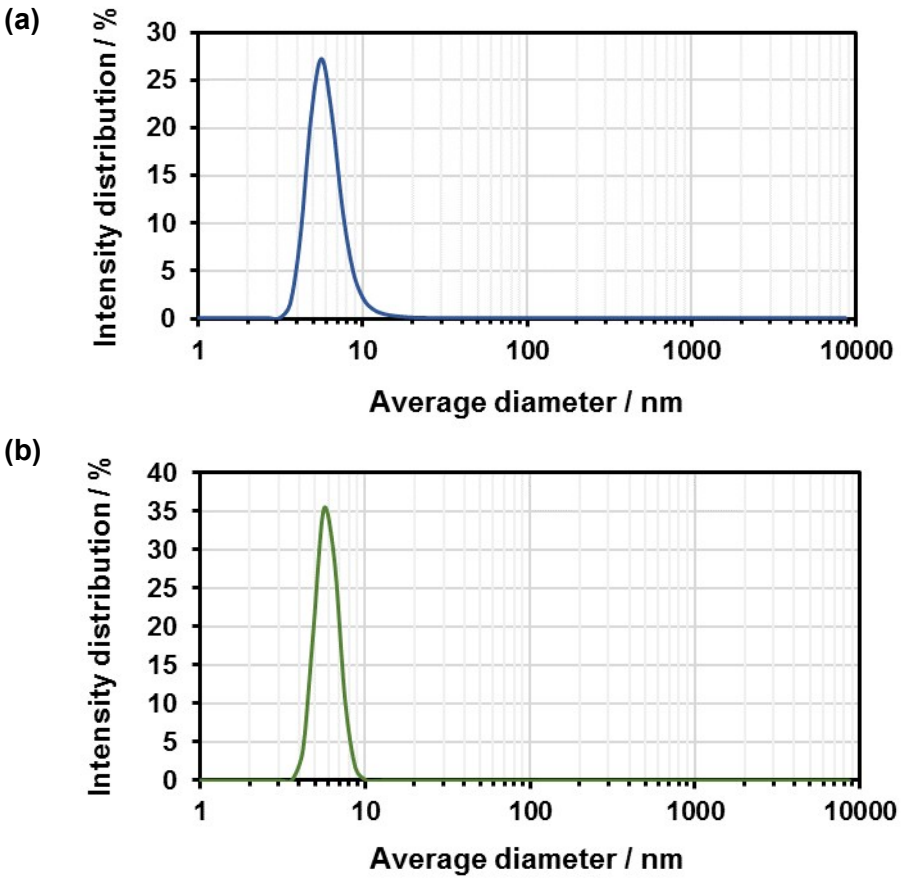

Figure S18. Number-average diameters of Gem-digly-P(OEGMA-co-MPDL) prodrugs **P2d** (a) and **P3d** (b) after solubilization in water. Note that number-average representation is shown here to highlight the most representative species (that is the soluble copolymer fraction).

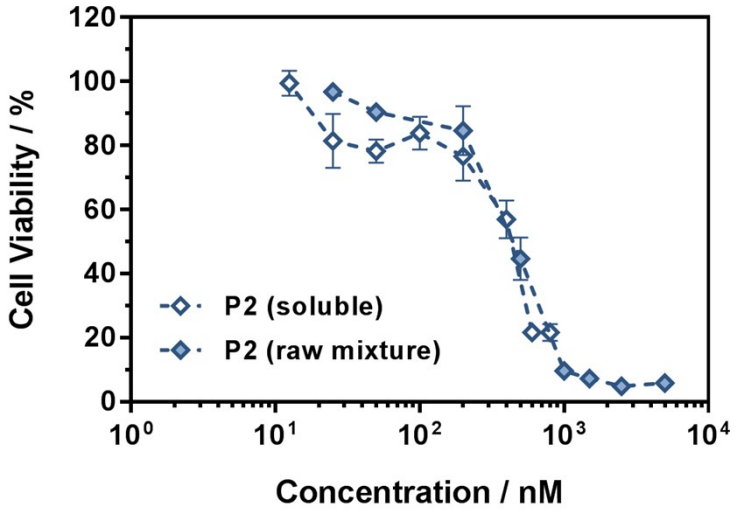

Figure S19: Cell viability (MTT test) with increasing concentrations of Gem-P(OEGMA-*co*-MPDL) (**P2**) either under the form of the purified soluble copolymer or the raw mixture (containing 8 wt.% nanoparticles) on A549 cells.

Table S1. Experimental Conditions and Macromolecular Properties of Gem-P(OEGMA-*co*-MPDL) Polymer Prodrugs **P3'** and **P3''**.

Prodrug	Alkoxyamine	Methacrylic ester	$f_{MPDL,0}$	Conv.[a] (%) / Time (h)	M_n[b] (g/mol)	$Đ$[b]	Drug loading (wt.%)
P3'	Gem-AMA-SG1	OEGMA	0.7	15 / 8	7 300	1.27	3.6
P3''	Gem-AMA-SG1	OEGMA	0.7	20 / 8	2 900	1.55	9.0

[a] OEGMA conversion determined by ^{1}H NMR. [b] Determined by SEC after precipitation.

Table S2. Predicted HLB of Gem-digly-$PMMA_4$ and Gem-digly-$PMMA_4$ from Marvin Sketch 18.10 using the Davies or the Griffin method.

Prodrug	Predicted HLB[a]	
	Davies method	Griffin method
Gem-digly-$PMMA_4$	18.23	11.83
Gem-$PMMA_4$	14.03	10.79

[a]Predicted using Marvin Sketch 18.10

Table S3. Characterization of Gem-P(OEGMA-*co*-MPDL) Nanoparticles.

Prodrug	D_z (nm)	PSD	%NP (wt. %)
P1	166	0.51	< 1
P2	146	0.13	8
P3	163[a]	0.19	16

[a] After 30 days, D_z = 157 nm, PSD = 0.21. After ultracentrifugation (40000 rpm, 4 h, 4 °C) and resuspension, D_z = 156 nm, PSD = 0.19.

Table S4. In Vitro Cytotoxicity (IC_{50}) of Gem-Based Polymer Prodrugs Against A549 and MiaPaCa-2 Cancer Cells.

Prodrug	F_{MPDL} (mol. %)	A549 IC_{50} (μM)	MiaPaCa-2 IC_{50} (μM)
P1	6	0.30	0.13
P2	12	0.88	0.45
P3	25	2.14	1.07
P1d	7	0.04	0.03
P2d	11	0.11	0.17
P3d	22	0.40	0.34
P4	10	-	-
P5	19	-	-
P6	29	-	-
P4d	7	~1	0.92
P5d	12	-	2.11
P6d	29	-	3.55